- Technical Paper -

SEISMIC PERFORMANCE OF COMPOSITE *EWECS* COLUMNS USING SINGLE H-STEEL

FAUZAN[*1], Hiroshi KURAMOTO[*2] and Ki-Hyung KIM[*3]

ABSTRACT

The results of tests conducted on four Engineering Wood Encased Concrete-Steel (EWECS) composite columns using single H-steel are presented. The columns were tested under constant axial load and lateral load reversals. The main test variable was the type of column-stub connection. The results indicated that EWECS columns had excellent hysteretic behavior without severe damage, even at large story drift of 0.04 radian. Moreover, the type of column-stub connection consisting of woody shell and wood panel attached to stub showed high performance in both capacity and damage limit of the columns.

Keywords: concrete-encased steel, composite structures, column, woody shell, seismic test

1. INTRODUCTION

Engineering Wood Encased Concrete-Steel (EWECS) column is a new composite structural system consisting of concrete encased steel (CES) core and an exterior woody shell, as shown in Fig. 1. Both economical and structural benefits are realized from this type of composite column due to the use of woody shell as column cover. During construction, the woody shell acts as forming for the composite column, decreasing the labor and materials required for construction and, consequently, lowering the construction cost. In the structural point of view, the shell improves the structural behavior of the column through its action to provide core confinement and resistance to bending moment, shear force and column buckling [1]. These advantages make EWECS columns possible to apply to actual structures as an alternative to steel reinforced concrete (SRC) columns, which have weaknesses due to difficulty in constructing both steel and reinforced concrete (RC) [2][3].

In our previous study [1], the structural behavior of a EWECS column using cross shape section of double H-steel had been investigated and it was found that the EWECS column had a stable spindle-shaped hysteresis characteristic without capacity reduction until the maximum story drift, R of 0.05 radian. The use of double H-Steel is effective for columns subjected to bending moments and shear forces in two directions, such as those in the frame structures. Furthermore, EWECS columns using single H-steel, shown in Fig. 1b, are being developed to apply to columns in one-way moment frame connected with shear wall in the orthogonal directions.

This paper presents the results of an experimental study on the performance of EWECS composite columns using single H-steel, subjected to both constant axial load and lateral load reversals that simulated earthquake loading. The type of column-stub connection was selected as the primary experimental parameter in this study. The performance of the columns was evaluated in terms of hysteresis loops, failure mode, axial deformation and curvature.

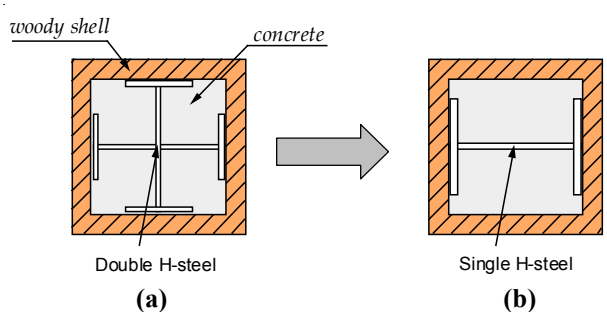

Fig.1 Cross-sections of EWECS columns

*1 Graduate Student, Dept. of Arch. & Civil Eng., Toyohashi Univ. of Technology, MSc.E., JCI Member
*2 Associate Prof., Dept. of Arch. & Civil Eng., Toyohashi Univ. of Technology, Dr.E., JCI Member
*3 Graduate Student, Dept. of Arch. & Civil Eng., Toyohashi Univ. of Technology, JCI Member

2. EXPERIMENTAL PROGRAMS

2.1 Specimens and Materials Used

Three composite column specimens of which the scale is about two-fifth, were tested. The dimensions and details of the specimens are shown in Fig. 2 and Table 1. Three types of woody shell connection at column-stub joints were constructed in this study, as shown in Fig. 3:

- Connection between woody shell and wood panel attached to stub (Specimen C3A)
- Connection between woody shell and concrete stub (Specimen C3B)
- Continuous woody shell connected with steel plates in the stub using bolts (Specimen C3C)

All specimens had a column with 1,600 mm height and 400 mm square section. The thickness of the woody shell was 45 mm and the steel encased in each column had a single H-section steel of 300x220x10x15 mm. The mechanical properties of the steel and the woody shell are listed in Tables 2 and 3, respectively. Normal concrete of 35 MPa was used for all specimens. The mix proportions and mechanical properties of the concrete are given in Table 4.

In manufacturing the specimens, the steel sections were accurately cut to size of the column and stub firstly. Then the steel plates, PL-9 were welded to the section as tie plates to prevent the local buckling of steel flanges and to confine the concrete core. Next, the woody shell panels were assembled to the column by using epoxy (Fig. 2).

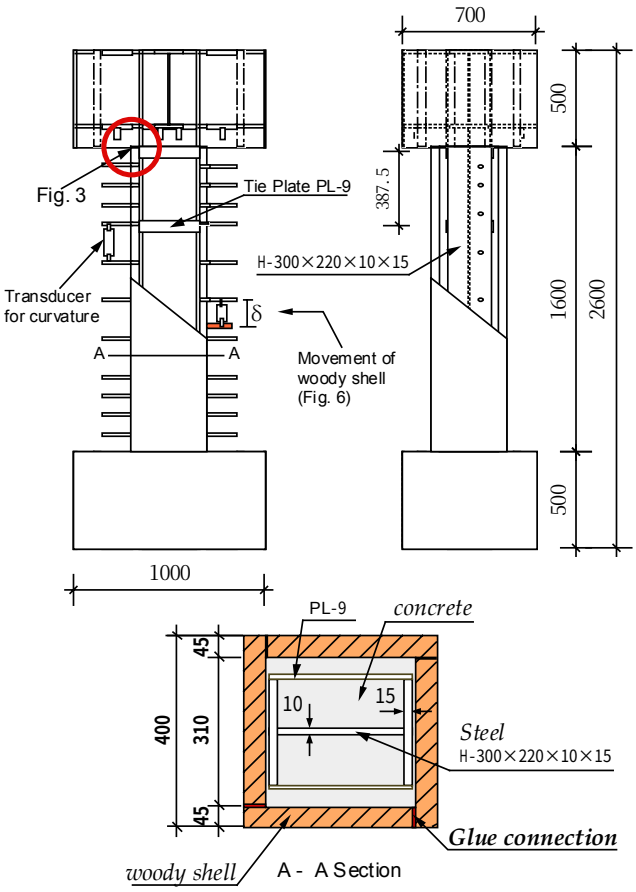

Fig.2 Test specimen

Finally, the concrete was cast into the column without additional formwork because the woody shell serves as mold forms for concrete placement.

Table 1 Test program

Specimen		C3A	C3B	C3C
Column -stub connections		Woody shell and wood panel attached to stub	Woody shell and concrete stub	Continuous Woody shell into stub
Woody Shell Thickness (mm)		45		
Concrete		Normal Concrete		
Steel	Built-in steel (mm)	H-300 x 220 x 10 x 15		
	Tie plate (mm)	PL-9		
Column Height: h (mm)		1600		
Cross section: b x D (mm)		400 x 400		
Axial Compression	N (kN)	1031		
	N/(b .D .σ_B)	0.17		

σ_B, uniaxial compressive strength of concrete

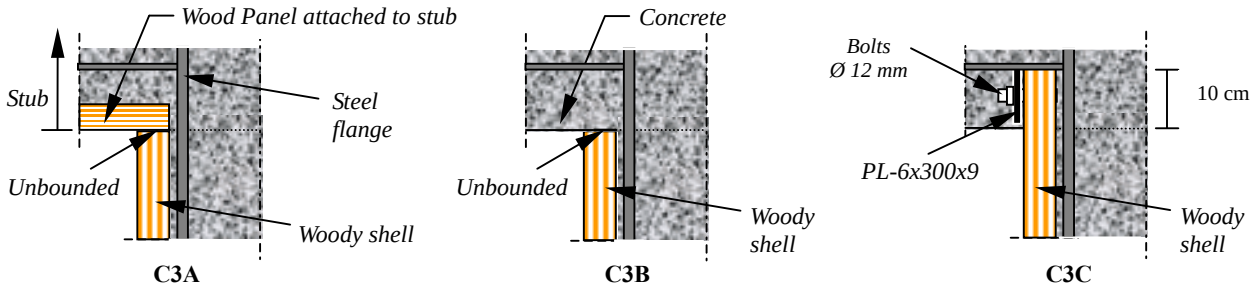

Fig.3 Types of column-stub connection

Table 2 Mechanical properties of steel

Steel	Elastic Modulus Es(GPa)	Yield Stress σy (MPa)	Notes
H-300x220x10x15	146.8	293.6	Flange
	156.7	313.3	Web
PL-9	146.8	293.6	Tie Plate

Table 3 Mechanical properties of woody shell

Woody shell panel (cm)	Wood type	[a] Comp. Strength σw (MPa)	Elastic Modulus Es (GPa)
40x160x4.5	Glue laminated pine wood	46.2	13.7

[a] the direction is parallel to axis of grain

Table 4 Mix proportions and mechanical properties of concrete

W/C (%)	S/(S+G) (%)	Slump (cm)	Unit weight (kg/m3)					Comp. Strength MPa
			Water (W)	Cement (C)	Sand (S)	Gravel (G)	Admixture (A)	
52	46.8	18	182	350	1060	408	3.5	35

2.2 Test Setup and Loading Procedures

The specimens were loaded lateral cyclic shear forces by a horizontal hydraulic jack and a constant axial compression of 1031 kN by two vertical hydraulics jacks, as shown in Photo 1. Considering the cross section of the woody shell, the applied axial force ratio, $N/(b.D.\sigma_B)$ for all specimens was 0.17, while using the core area, the ratio, $N/(b_c.D_c.\sigma_B)$ was 0.25.

The loads were applied through a steel frame attached at the top of a column that was fixed to the base. The two vertical jacks applying the constant axial compression were also used to keep the column top beam parallel to the bottom beam, so that the column would be subjected to anti-symmetric moments.

The incremental loading cycles were controlled by story drift angles, R, which was given by the ratio of lateral displacements to the column height, δ/h. In this experiment, the specimens were cyclically loaded twice for R of 0.005, 0.01, 0.015, 0.02, 0.03 and 0.04 radians, and once for that of 0.05 radian, respectively.

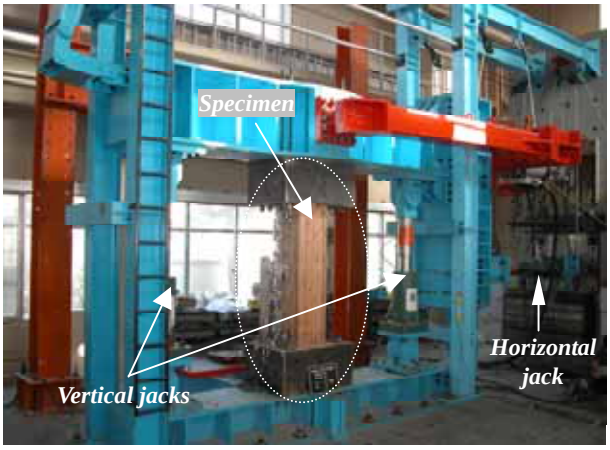

Photo 1 Loading apparatus

3. EXPERIMENTAL RESULTS AND DISCUSSIONS

3.1 Hysteresis Characteristics and Failure Modes

Shear versus story drift angle relationships of all specimens are given in Fig. 4. In this figure, the predicted flexural capacities calculated by fiber section analysis [1] are shown by dotted lines. The yield and maximum strengths and the corresponding story drift angles for each specimen are listed in Table 5. The yielding of each specimen was assumed when the first yielding of steel flange at the top and bottom of the columns was observed, which corresponds to a triangle mark on the shear versus story drift angle response (see Fig. 4). Crack modes of all specimens at R of 0.05 rad. are presented in Photo 2. Failure patterns of all specimens at column-stub joint after loading are shown in Photo 3.

From Fig. 4, it can be seen that all specimens showed ductile and stable spindle-shaped hysteresis loops without degradation of load-carrying capacity until story drift, R of 0.04 radian. The measured maximum flexural strengths fairly agreed with the calculated flexural strengths.

In Specimen C3A with column-stub connection consisting of woody shell and wood panel attached to stub, the first cracks in the woody shell occurred at around 30 cm away from the top of the column at story drift, R of about 0.032 rad. With an increase of the story drift, the cracks propagated along the column faces. Sink and uplift were observed significantly after R of 0.02 rad. at two opposite sides of both the top and bottom of the column due to different grain directions between the woody shell and the wood panel attached to stub. The hysteresis loops of this specimen showed excellent behavior without

strength degradation until the last cycle. The maximum capacity of 706.5 kN was reached at story drift, R of 0.05 rad.

For Specimen C3B with column-stub connection consisting of woody shell and concrete stub, the hysteresis curve showed a stable behavior with a little strength degradation after attaining the maximum capacity at R of 0.04 rad. The maximum capacity of this specimen was less than that of Specimen C3A.

Specimen C3C with continuous woody shell into stub showed high performance, with highest maximum capacity among the tested specimens. However, the brittle failure of the woody shell and severe damage of the concrete stub around the column-stub joints were observed significantly in this specimen after R of 0.03 rad.

Due to different column-stub connections, the test specimens showed different cracking patterns at the column faces, as shown in Photo 2. Up to story drift, R of 0.03 rad., no damage was observed in Specimen C3A and little crack occurred in Specimens C3B and C3C. However, the damage situations of the columns were different at the last story drift, R of 0.05 rad. At this stage, the most damage of the woody shell was observed in Specimen C3B, while Specimen C3A showed better performance in damage limit than the other two specimens.

The different failure modes at critical joint regions between column and stubs were also observed among these specimens. Sink and uplift occurred in Specimens C3A and C3B, while slip between woody shell and concrete stub (slip displacement) was observed in Specimen C3C, as shown in Photo 3. Specimen C3A had little damage at the column-stub joints due to the effect of sink and uplift that occurred at the joint regions. Meanwhile, the most damage of the woody shell at the joint region was observed in Specimen C3B due to the higher stiffness of concrete than woody shell. For Specimen C3C, the slip between woody shell and concrete stub at the joints caused the crush of concrete stub around the joint regions.

Figure 5 shows the comparison of sink, uplift and slip displacements of the woody shell at each story drift angle for all specimens. It can be seen from the figure that Specimen C3A had the highest value of sink and uplift displacements compared with the other specimens. For this specimen, the maximum sink of 8.4 mm and uplift of 11.3 mm were reached at R of 0.04 rad.

Figure 6 compares the movement of the woody shell from the CES core until the story drift, R of 0.03 rad. for all specimens. The values were obtained by measuring the displacement between

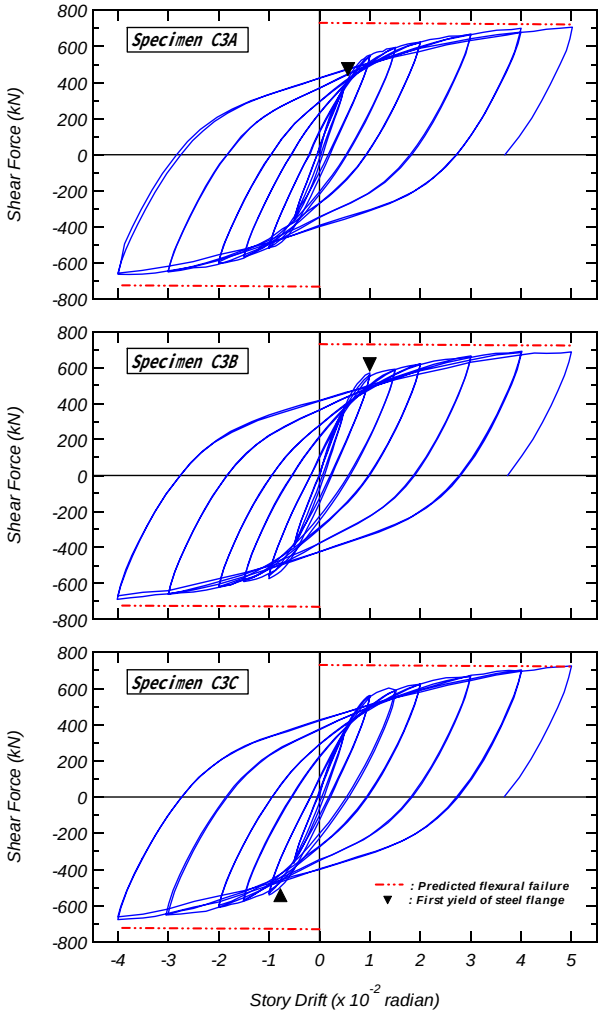

Fig.4 Shear force - story drift relationships

Table 5 Measured strength

Specimen	at Yielding		at the Max. Capacity	
	Qy (kN)	Ry (rad.)	Qmax (kN)	Rmax (rad.)
C3A	422.5	0.00571	706.5	0.05
C3B	570	0.01002	690	0.04
C3C	-498	-0.00768	725	0.05

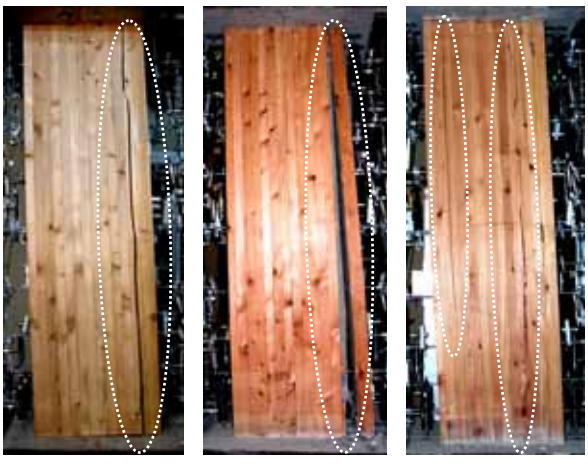

C3A C3B C3C

Photo 2 Crack modes of specimens at R = 0.05 rad. after loading

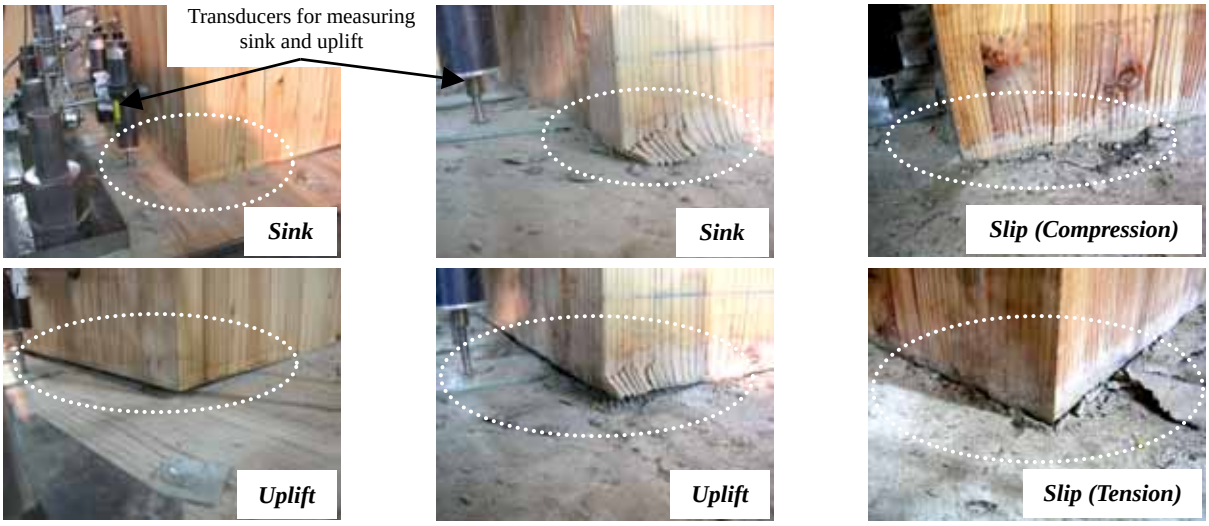

Photo 3 Failure patterns at column-stub joint after loading

the CES core and the woody shell using vertical transducers installed at the encased steel and the woody shell at the top, middle and bottom of the column, as shown in Fig. 2. From Fig. 6, it can be seen that the movement of the woody shell from the CES core at the top and middle of the columns was relatively small for all specimens. The smallest movement of the woody shell was observed in Specimen C3A due to the effect of sink and uplift at column-stub joints. In Specimen C3B, on the other hand, the highest movement occurred at the middle of the column, possibly due to the deterioration of the woody shell at the column-stub joints after R of 0.01 rad.

By comparing among these specimens, it is revealed that all the specimens had excellent hysteretic behavior with almost the same maximum capacity. However, Specimen C3A showed better performance in propagation of cracks in the woody shell and had the smallest movement of the woody shell than the other two specimens. This means that the EWECS columns with column-stub connection consisting of woody shell and wood panel attached to stub exhibited excellent performance in both capacity and damage limit of the composite columns.

It was also observed from this study that the woody shell contributed to flexural strength until large story drift, R of 0.05 rad. for Specimens C3A and C3C, although the cracks appeared along the column faces after R of 0.03 rad. (see Fig. 4 and Photo 2).

Extracting the woody shell after testing, it was observed for all specimens that the in-filled concrete had crushed in flexure at both the top and bottom of the column and there was no local buckling occurred at the encased steel.

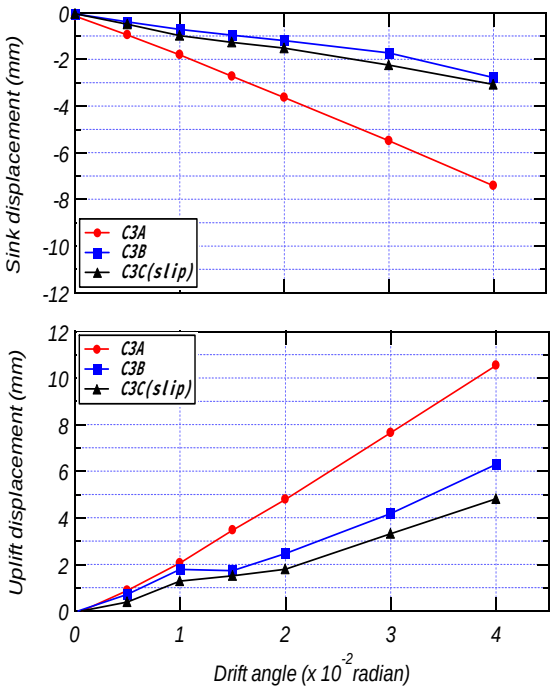

Fig.5 Sink and uplift displacements of woody shell at column-stub joint

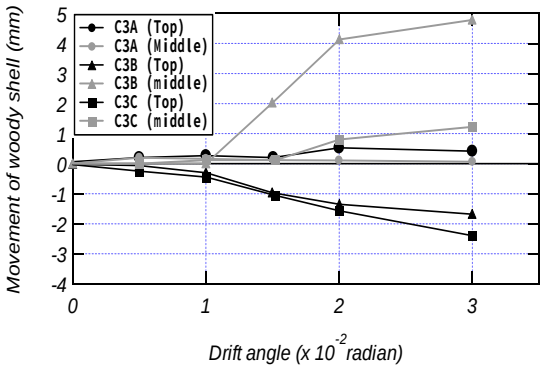

Fig.6 Movement of woody shell

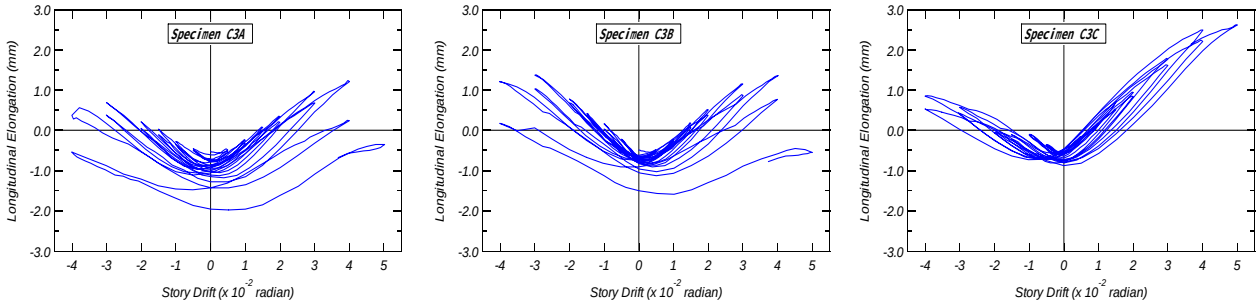

Fig.7 Axial deformation

3.2 Axial Deformation

Figure 7 shows the longitudinal elongation versus drift angle relationships of all specimens. The elongations of the specimens were recorded from two vertical transducers installed at the mid-height of the column.

As seen in Fig. 7, Specimens C3A and C3B had symmetrical patterns of axial deformation, while the deformation of Specimen C3C was unsymmetrical, possibly due to the early failure of bolted woody shell connection at the east side of the stub after R of 0.01 rad. Specimens C3A and C3B reached almost the same maximum elongation of around 1.5 mm at R of 0.04 rad., while Specimen C3C reached the maximum elongation of 2.5 mm at R of 0.05 rad.

3.3 Curvature Distribution

Figure 8 shows the curvature distributions along the column height at R of 0.005, 0.01 and 0.015 radians for Specimen C3A, which is almost similar for the other two specimens (C3B and C3C). The values were obtained from transducers installed on the two opposite sides along the column height, as shown in Fig. 2.

As can be seen in Fig. 8, the distribution of curvature was almost identical at each story drift angle in which the highest curvature occurred at both the top and bottom of the column. The curvatures increased with an increase of story drift angle and the maximum curvature of approximately 1.15×10^{-4} was obtained at R of 0.015 rad.

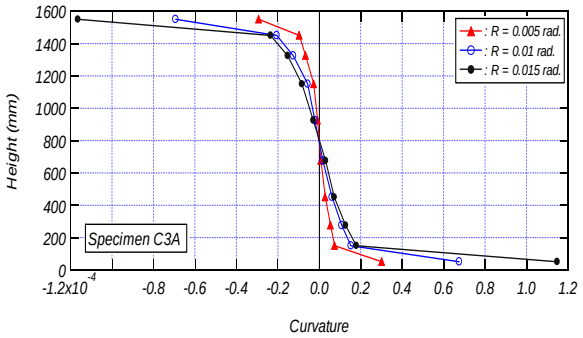

Fig.8 Curvature distribution

4. CONCLUSIONS

Based on the experimental study presented here, the following conclusions can be drawn:

(1) EWECS columns using single H-steel had excellent structural performance without severe damage, even at large story drift, R of 0.04 rad.

(2) The woody shell contributed to flexural capacity until large story drift, R of 0.05 rad., although cracks appeared at the column faces after R of 0.03 rad.

(3) EWECS column with column-stub connection consisting of woody shell and wood panel attached to stub showed excellent performance in both capacity and damage limit of the composite column due to the effect of sink and uplift of the woody shell that occurred at the joint regions.

REFERENCES

[1] Fauzan, Kuramoto, H., Shibayama, Y. and Yamamoto, T., “Structural Behavior of Engineering Wood Encased Concrete-Steel Composite Columns,” Proceedings of the Japan Concrete Institute (JCI), Vol.26, No.2, 2004, pp. 295-300.

[2] Kuramoto, H., Takahashi, H. and Maeda, M., “Feasibility Study on Structural Performance of Concrete Encased Steel Columns using High Performance Fiber Reinforced Cementitious Composites,” Summaries of Technical Papers of Annual Meeting, AIJ, Vol.C-1, 2000, pp. 1085–1088 (in Japanese).

[3] Kuramoto, H., Adachi, T. and Kawasaki, K., “Behavior of Concrete Encased Steel Composite Columns Using FRC,” Proceedings of Workshop on Smart Structural Systems Organized for US-Japan Cooperative Research Programs on Smart Structural Systems (Auto-Adaptive Media) and Urban Earthquake Disaster Mitigation, Tsukuba, Japan, 2002, pp. 13-26.